Single-photon-induced phonon blockade in a hybrid spin-optomechanical system

Li-Li Zheng, Tai-Shuang Yin,[*] Qian Bin, Xin-You Lü,[†] and Ying Wu[‡]

School of Physics, Huazhong University of Science and Technology, Wuhan 430074, China

We explore the photon-controlled phonon statistics in a hybrid spin-optomechanical system. Here the proposed phonon blockade is based on the nonlinearity of system induced by the strong spin-mechanical coupling. Our approach involves introducing an ancillary quadratic optomechanical coupling (i.e., the cavity field quadratically coupled to mechanical motion) and simultaneously considering the cavity field with a single photon. By injecting the auxiliary photons, one can not only enhance the spin-resonator interaction, but also realize fully switchable phonon blockade. This work offers an approach to manipulate phonon statistics with photons, which should inspire the engineering of new single-phonon quantum devices and have potential applications in the future hybrid photon-phonon quantum networks.

I. INTRODUCTION

The last decade has witnessed spectacular progress in the field of cavity optomechanics, exploring the nonlinear interaction between the electromagnetic and mechanical systems [1–3]. In particular, with the significant development of nanomechanical fabricating technologies, the mechanical modes even with megahertz frequency could be experimentally cooled to their quantum ground state [4–7]. This makes it possible for the observation of mechanical quantum effects [8–26] and applications in quantum information processing for the mechanical system [27]. One of the important quantum effects is phonon blockade, which could be induced by a large mechanical nonlinearity. In analogy to photon blockade [28–33], phonon blockade is a phenomenon in which the appearance of one phonon prevents the excitation of the second phonon in a nonlinear mechanical oscillator. Phonon blockade has been studied in a nanomechanical resonator coupled to a qubit in the dispersive and resonant regimes [8–10] or an intrinsic two-level system defect [11]. It is also demonstrated in a quadratically coupled optomechanical system (OMS) [12–15].

Recently, remarkable advances have been made towards single-photon technologies. For example, many alternative single-photon sources, e.g., quantum dots [34–36], single atoms [37,38], trapped ions [39], color centers in diamond [40], have been employed to generate single photons. In addition, single-photon detection has been demonstrated by exploiting cavity-QED design [41] or using cross-phase modulation [42]. Based on these achievements, single photons provide a promising integration option for connecting distinct components [35], which are required for establishing quantum networks. Furthermore, it also promotes the exploration of associated quantum devices, including

single-photon transistors [43], single-photon routers [44], single-photon switches [45], and a single-phonon source triggered by a single photon [46] and single-photon-induced entanglement and quantum phase transition [47,48].

Associating single-photon technologies with mechanical quantum effects, here we propose a hybrid quantum model to explore the photon-controlled phonon statistics. Specifically, the hybrid quantum model consists of a Rabi model (a spin coupled to mechanical motion) coupled to the ancillary cavity modes (a_e and a_o) via a quadratic optomechanical coupling [49,50]. The single-photon-induced phonon blockade is achieved by the single-photon-enhanced spin-resonator interaction. This enhancement is induced by combining the quadratic optomechanical coupling (the cavity field quadratically coupled to mechanical motion) with the cavity field that is simultaneously mediated by a single photon. More interestingly, the present phonon blockade is fully switchable by injecting the auxiliary photons. Specifically, the presence of the single photon only in the ancillary mode a_e with zero photon in a_o can enable the phonon blockade phenomenon. However, the coexistence or nonexistence of a single photon in both ancillary modes a_e and a_o will switch off this phenomenon. When being extended to the case of multiple photons, the switchable quantum behavior for the phonons is determined by the difference between the number of photons in the two ancillary modes. Clearly, this controllable characteristic utilizes the combined effect of two ancillary cavity modes instead of only one ancillary cavity mode.

Note that our approach is different from the previous proposals, which employ qubit-induced mechanical nonlinearity in a coupled qubit-resonator system [8–10] or the optically induced nonlinearity by strongly driving the cavity [11–15]. Particularly, the phonon blockade has been proposed in two recent works [14,15], both of which are based on the optomechanical nonlinearity between photons and phonons. In our proposal, however, the phonon blockade is induced by the nonlinearity between the mechanical mode and a two-level system, which is physically different from that in Refs. [14,15]. Besides this, the previous studies apply

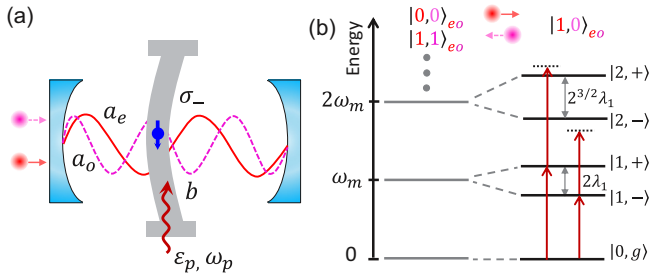[*]taishuangyin@163.com
[†]xinyoulu@hust.edu.cn
[‡]yingwu2@126.com

FIG. 1. (a) Schematic illustration of a hybrid model including a Rabi model quadratically coupled to ancillary cavity modes $a_l(l = e, o)$ with the "membrane-in-the-middle" configuration. Here the subscript e (o) denotes the field mode a_e (a_o) with the even (odd) number of half wavelengths in the full cavity, respectively. The Rabi model consists of a two-level system σ_- (e.g., a nitrogen-vacancy center spin) interacting with the mechanical mode b. A weak probe field with driving frequency ω_p and strength ε_p is applied into the mechanical oscillator. (b) Energy-level diagram of the single-photon-induced spin-oscillator system. The corresponding dressed states are $|m, \pm\rangle$. $|m\rangle$ and $|g\rangle$ denote the eigenstates of the phonon number and the ground state of the two-level system, respectively. Here the ancillary modes a_l are prepared into a two-mode Fock state $|n_e, n_o\rangle_{eo}$ ($n_e = n_o + n$), and we focus on the case of $n_l, n = 0, 1$.

a strong external field to coherently drive the cavity such that the nonlinear interaction between photons and phonons could reach the desired coupling strength [14,15]. Instead of using the coherent driving field due to the weak quadratic coupling in an OMS, our work exploits the ancillary cavity modes with a single photon in the presence of a relatively strong quadratic coupling, which could be used to achieve the photon-dependent nonlinear coupling. This provides a unique superiority for the realization of photon-controlled phonon statistics, which could realize single-photon-induced phonon blockade. Overall, compared with these works [8–15], first, our approach realizes single-photon-manipulated phonon blockade by introducing an ancillary quadratic OMS. Second, the realized phonon blockade here is completely switchable, which can be controlled by the photon numbers of the two ancillary cavity modes. Third, taking advantage of available single-photon technologies, the switchable quantum behavior for the phonons may inspire the engineering of new single-phonon quantum devices and could be applied into various phononic [51] or hybrid photon-phonon quantum networks [27,52–55].

This paper is organized as follows: In Sec. II we describe the hybrid spin-optomechanical system and derive the Hamiltonian with the photon-dependent nonlinear coupling between the mechanics and a two-level system. In Sec. III we demonstrate the photon-controlled phonon statistics featured by the second-order correlation function, and the switchable behavior of the phonon blockade is shown. In addition, we also discuss the experimental challenge for the feasibility of our proposal. Conclusions are given in Sec. IV.

II. THEORETICAL MODEL

Figure 1(a) gives the schematic diagram of a hybrid quantum model: a Rabi model coupled to the ancillary cavity

modes via a quadratic optomechanical coupling. The system Hamiltonian reads ($\hbar = 1$)

$$H_s = H_{an} + H_{rm} - \sum_{l=e,o} g_l a_l^\dagger a_l (b + b^\dagger)^2, \quad (1)$$

where a_l ($a_l^\dagger$) and b ($b^\dagger$) are the annihilation (creation) operators of the ancillary cavity modes and mechanical mode, respectively. The ancillary cavity, with the Hamiltonian $H_{an} = \sum_{l=e,o} \omega_l a_l^\dagger a_l$, contains the field mode a_e (or a_o) with the even (odd) number of half wavelengths in the full cavity, which quadratically couples to the mechanical mode b with coupling strength $g_e = g$ (or $g_o = ge^{i\pi}$) [50]. The coupling strengths g_e and g_o have the opposite sign. This originates from the fact that the second derivative of the frequency for the two cavity modes a_e and a_o with respect to the mechanical displacement is opposite. The Hamiltonian H_{rm} is $H_{rm} = \frac{\Omega}{2}\sigma_z + \omega_m b^\dagger b + \lambda(b^\dagger + b)\sigma_x$, where σ_z and σ_x are the Pauli operators for a two-level system, and λ denotes the coupling strength between the two-level system (with transition frequency Ω) and mechanical mode (with frequency ω_m).

The proposed hybrid model could be realized in a quadratically coupled optomechanical system with the "membrane-in-the-middle" configuration [49,50]. A thin dielectric membrane is located at a node (or antinode) of the intracavity standing wave. Then the cavity field will quadratically couple to the mechanical motion. The Rabi model can be implemented by coupling the mechanical oscillator to a two-level system, i.e., the nitrogen-vacancy (NV) center spin embedded in diamond [56–58]. Specifically, due to the strain yielded by the flex of diamond membrane, the diamond lattice could directly couple to the spin triplet states in the NV electronic ground state.

In the following, we consider the ancillary modes are prepared into a two-mode Fock state $|n_e, n_o\rangle_{eo}$ ($n_e = n_o + n$ and $n_e, n_o, n = 0, 1, \dots$). In this case, the number operator $a_l^\dagger a_l$ can be replaced by an algebraic number n_l. Then, applying a squeezing transformation $b = b_n \cosh(r_n) + b_n^\dagger \sinh(r_n)$ with $r_n = -\frac{1}{4}\ln(1 - 4ng/\omega_m)$, the Hamiltonian (1) is expressed as

$$H_n = \frac{\Omega}{2}\sigma_z + \omega_n b_n^\dagger b_n + \lambda_n(b_n^\dagger + b_n)\sigma_x + C_n, \quad (2)$$

where $\omega_n = \exp(-2r_n)\omega_m$ and $\lambda_n = \exp(r_n)\lambda$ are the transformed mechanical frequency and spin-resonator coupling, respectively, and $C_n = \sum_{l=e,o} n_l \omega_l + [\exp(-2r_n) - 1](\omega_m/2)$ is the constant term. It clearly shows that the present hybrid quantum model is essentially equivalent to a photon-dependent Rabi model. Note that when the membrane cannot be placed exactly at the node or antinode of the two cavity modes, there will be some residual linear optomechanical coupling between the cavity modes and the motion. This linear coupling can be included in the transformations leading to Eq. (2), but its effect in the dynamics is small and can be neglected. Under the conditions of $\omega_n \approx \Omega$ and $\omega_n \gg \lambda_n$, the antirotating terms can be neglected under the rotating-wave approximation (RWA). The Hamiltonian (2) is reduced to the photon-dependent Jaynes-Cummings model,

$$H_{n'} = \frac{\Omega}{2}\sigma_z + \omega_n b_n^\dagger b_n + \lambda_n(b_n^\dagger \sigma_- + b_n \sigma_+), \quad (3)$$

where σ_+ and σ_- are the raising and lowering operators of the two-level system, and the constant term C_n has been neglected.

Here we assume that the mechanical oscillator is coupled to a squeezed vacuum reservoir [59–62]. In principle, it could be realized by introducing an ancillary cavity mode a_c, which is driven by a strong red-detuned laser field and linearly couples to the mechanical motion. Moreover, the ancillary mode a_c is initially in a squeezed vacuum environment by interacting with a broadband-squeezed vacuum field (with the squeezing parameter r_e and reference phase Φ_e) [63]. When the decay rate of the ancillary mode a_c is much larger than the linearized optomechanical coupling between modes a_c and b, the ancillary mode adiabatically follows the dynamics of mechanical mode b. Then this squeezed vacuum bath could be transferred to the mechanical mode. Under the ideal parameter conditions, the amplified thermal noise due to the squeezed effect can be suppressed completely. Qualitatively, this result can be understood from the phase matching [63,64]. In the following discussion and calculations, we treat the mechanical mode in this ideal parameter conditions. Other alternative strategies could also be exploited to eliminate the amplified noise, such as the "transitionless" driving (TD) protocols [65].

Including the dissipation caused by the system-bath coupling, the dissipative dynamics of the hybrid quantum system in terms of the mechanical mode b_n is described by the master equation

$$\dot{\rho} = -i[H_{\text{tot}}, \rho] + \kappa(n_{\text{th}} + 1)\mathcal{D}[b_n]\rho$$
$$+ \kappa n_{\text{th}}\mathcal{D}[b_n^\dagger]\rho + \gamma\mathcal{D}[\sigma_-]\rho, \quad (4)$$

where $\mathcal{D}[o]\rho = o\rho o^\dagger - \frac{1}{2}(o^\dagger o\rho + \rho o^\dagger o)$ is the standard Lindblad superoperator, κ and γ is the decay rate of the mechanical oscillator and the two-level system, respectively, and n_{th} is the thermal phonon occupation number with $n_{\text{th}} = [\exp(\hbar\omega_m/k_B T) - 1]^{-1}$ where T is the temperature of the thermal reservoir.

III. PHONON BLOCKADE

To exhibit how the behavior of the phonons is controlled by the ancillary photons, we investigate the statistical properties of the phonons, which are characterized by the second-order correlation function in the steady state

$$g^{(2)}(\tau) = \text{Lim}_{t\to\infty}\frac{\langle b_n^\dagger(t)b_n^\dagger(t+\tau)b_n(t+\tau)b_n(t)\rangle}{\langle b_n^\dagger(t)b_n(t)\rangle^2}. \quad (5)$$

Note that the timescale t for reaching the steady state in Eq. (5) is about $t \sim 1/\kappa$. It has to be fast on the timescale of the cavity decay rate so that the photon that induces the phonon blockade will not leak out of the cavity. For the observation of phonon blockade effects, we consider a weak probe field (with frequency ω_p and strength ε_p) applied into the mechanical oscillator and the Hamiltonian is $H_p = \varepsilon_p(b^\dagger e^{-i\omega_p t} + be^{i\omega_p t})$. Then the total Hamiltonian, including the probe field, is

$$H_{\text{tot}} = H_n + \varepsilon_p[\cosh(r_n)b_n^\dagger e^{-i\omega_p t} + \sinh(r_n)b_n^\dagger e^{i\omega_p t} + \text{H.c.}]. \quad (6)$$
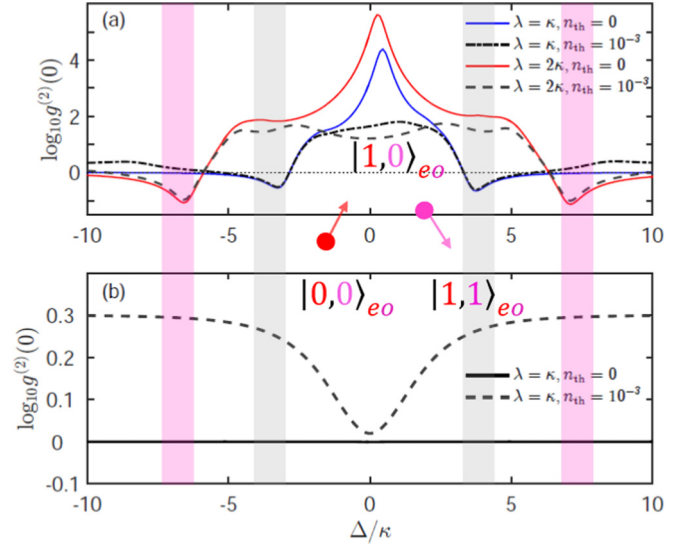

FIG. 2. The steady-state equal-time second-order correlation function $\log_{10}g^{(2)}(0)$ versus the detuning $\Delta/\kappa = (\omega_n - \omega_p)/\kappa$ with the total Hamiltonian H_{tot}. Panels (a) and (b) correspond to the case of $n = 1$ and $n = 0$, respectively. The system parameters we take are $\gamma = 0.1\kappa$, $\omega_m = 2300\kappa$, $\Omega = 200\kappa$, $g = 0.2481\omega_m$, $\varepsilon_p = 0.1\kappa$.

Under the conditions of $\omega_p \approx \omega_n$, Ω and $\omega_n \gg \lambda_n, \varepsilon_p \sinh(r_n)$, the effective Hamiltonian can be expressed as $H_{\text{eff}} = H_{n'} + \varepsilon_p \cosh(r_n)(b_n^\dagger e^{-i\omega_p t} + b_n e^{i\omega_p t})$ under the RWA, where $H_{n'}$ is given by Eq. (3). To show the quantum property triggered by a single photon, we focus on the case of $n_l = 0, 1$, which leads to $n = 0, 1$.

In Fig. 2 we calculate the steady-state equal-time second-order correlation function $g^{(2)}(0)$ versus the detuning $\Delta/\kappa = (\omega_n - \omega_p)/\kappa$ by numerically solving the master equation in Eq. (4) with the total Hamiltonian H_{tot}. Figures 2(a) and 2(b) correspond to the case of $n = 1$ and $n = 0$, respectively. For $n = 1$, it clearly shows that the phonon blockade can be obtained in the vicinity of the optimal detuning $\Delta = \pm\lambda_1$. This phenomenon can be illustrated by the energy-level diagram in Fig. 1(b), where $|m, \pm\rangle$ are the dressed states for the single-photon-induced spin-oscillator system. $|m\rangle$ and $|g\rangle$ denote the eigenstates of the phonon number and the ground state of the two-level system, respectively. If the driving laser is on resonance with the $|0, g\rangle \to |1, \pm\rangle$ transition, $\Delta = \pm\lambda_1$, the same $|1, \pm\rangle \to |2, \pm\rangle$ transition is detuned and will be suppressed for $\lambda_1 \gg \kappa$ and $\lambda_1 \gg \gamma$. In contrast with Fig. 2(a), $g^{(2)}(0)$ equals 1 for $n_{\text{th}} = 0$ in Fig. 2(b). Physically, this is due to the large frequency detuning and weak coupling between the atom and mechanical oscillator for $n = 0$, which results in the decoupling of the two subsystems. In addition, we also plot $g^{(2)}(0)$ in the presence of the thermal noise $n_{\text{th}} = 10^{-3}$, which can be seen from the dash-dotted line and dash line in Fig. 2(a) and dash line in Fig. 2(b). It's shown that the thermal noise will destroy the phonon blockade to some extent. By comparing with the two cases of $n = 1$ and $n = 0$, one could obtain that the statistical properties of the phonons can be controlled by the ancillary photons. More importantly, this controlled behavior is completely switchable via the ancillary photons. Specifically, when the ancillary
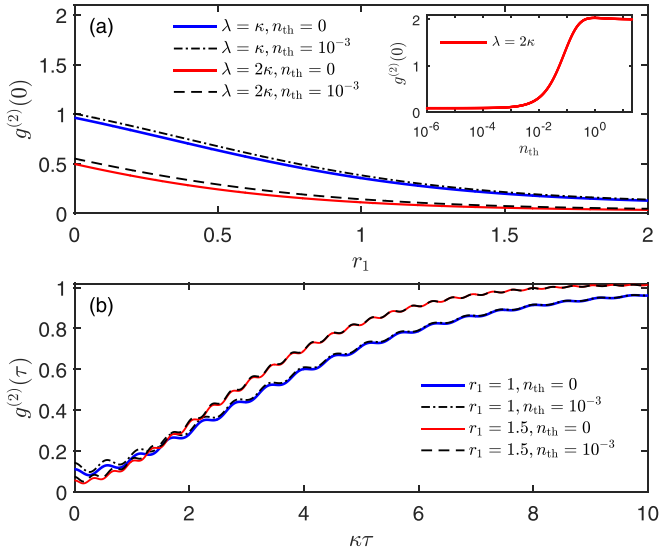
FIG. 3. (a) The equal-time second-order correlation function $g^{(2)}(0)$ versus the squeezing parameter r_1 ($n = 1$) and (b) the second-order correlation function $g^{(2)}(\tau)$ as a function of the scaled time delay $\kappa\tau$, both of which are obtained by numerically solving the master equation in Eq. (4) with the Hamiltonian H_{eff} and in the case of mechanical resonance $\Delta = \pm\lambda_1$. The system parameters are $\gamma = 0.1\kappa$, $\varepsilon_p = 0.1\kappa$, and (b) $\lambda = 2\kappa$.

modes are initially in the state $|0,0\rangle_{eo}$, there is no phonon blockade. Then if one photon ($n_e = 1$) is injected into the cavity, i.e., $|1,0\rangle_{eo}$, the phonon blockade can occur. However, if another photon ($n_o = 1$) is subsequently injected into the cavity, $|1,1\rangle_{eo}$, the phonon blockade will disappear. Thus, the single-photon-induced phonon blockade is fully switchable via the ancillary photons, $|0,0\rangle_{eo} \rightarrow |1,0\rangle_{eo} \rightarrow |1,1\rangle_{eo}$. Clearly, this switchable behavior comes from the combined effect of two ancillary cavity modes; namely, this behavior is impossible with only one ancillary cavity mode. In addition, when being extended to the case of multiple photons (i.e., $n_e, n_o > 1$), the switchable quantum behavior for the phonons is determined by the difference of the photon numbers in the two ancillary modes. When the photon numbers in the two ancillary modes are the same, $n_e = n_o$, the phonon blockade is switched off. When the ancillary photons are injected to lead to a difference, $n_e > n_o$, the phonon blockade is switched on. Essentially, the case for multiple photons can also be applied to demonstrate the obtained result in a similar approach. Thus, this situation isn't presented here. The above results demonstrate that our work provides a promising approach for performing the photon-controlled-phonon manipulations with currently developed quantum technologies. Combined with single-photon technologies, these manipulations might be applied into various phononic or hybrid quantum networks.

In Fig. 3(a) we plot $g^{(2)}(0)$ versus the squeezing parameter r_1 ($n = 1$) by numerically solving the master equation in Eq. (4) with the Hamiltonian H_{eff} and in the case of mechanical resonance $\Delta = \pm\lambda_1$. It can be seen that with the increase of r_1, the antibunching effect [$g^{(2)}(0) < 1$] of the phonons is gradually strengthened and the phonon blockade [$g^{(2)}(0) \rightarrow 0$] can be observed under relatively strong squeezing parameters. This demonstrates that the desired quantum

effect of the phonons could be yielded by adjusting the system parameters. In Fig. 3(b) we plot the correlation function $g^{(2)}(\tau)$ as a function of the scaled time delay $\kappa\tau$. First, the curves with different values of r_1 ($n = 1$) show that $g^{(2)}(0) < g^{(2)}(\tau)$ accompanied by slight oscillations. Additionally, we note that $g^{(2)}(\tau)$ approaches one, as expected. This indicates that the probability of two-phonon excitations at the same time ($\tau = 0$) is smaller than that at a different time ($\tau > 0$). Therefore, the resonant excitations from the ground state to the doubly excited state are suppressed. Moreover, we plot $g^{(2)}(0)$ and $g^{(2)}(\tau)$ when the thermal noise is $n_{\text{th}} = 10^{-3}$, as shown in Figs. 3(a) and 3(b). Compared with the case of $n_{\text{th}} = 0$, the phonon blockade effect is relatively weakened. To fully demonstrate this, we present $g^{(2)}(0)$ as a function of the thermal phonon occupation number n_{th} [see the inset of Fig. 3(a)]. It can be seen that the thermal noise has a significant effect on phonon blockade. When $n_{\text{th}} < 10^{-3}$, a strong phonon blockade can be observed. When n_{th} reaches 0.053, the phonon blockade will disappear. For the feasibility of the proposal, when choosing a gigahertz-frequency mechanical resonator [57,66], the environment temperature T needs to be below 16 mk. Thus, to better observe the desired phonon blockade, it requires cooling the mechanical resonator to low temperature [4–7], which could be realized by optimizing the fabrication and flexibility of the individual devices for the future experiments.

Note that there still exists an experimental challenge for the feasibility of our proposal since a relatively large quadratic optomechanical coupling (i.e., $g \approx \omega_m/4$) has been used in our calculations. The quadratic optomechanical coupling $g = \frac{1}{2}\omega_l''(0)x_{\text{zpf}}^2$ (x_{zpf} being the mechanical zero fluctuation) is typically weak, and its enhancement would require substantial improvements to the strength $\omega_l''(0)$, the membrane's optical absorption and the membrane's mechanical properties [49]. Importantly, these improvements could expand the application of quadratic optomechanics in the quantum realm, i.e., the quantum nondemolition measurement of the phonon number [67–69]. Fortunately, many efforts have been devoted to increase the quadratic optomechanical coupling. For example, related proposals involve using a fiber-based cavity with smaller and slighter membranes [70], for which the value of $\omega_l''(0)$ is significantly increased to about 20 GHz/nm². Other approaches also explore the possibility of achieving the strong-coupling regime of quadratic optomechanics, including the proposal for a near-field optomechanical system [71], the tunable superconducting circuit [72], or the utilization of optical parametric amplification [73]. Therefore, with the experimental flexibility in the future, it is possible to reach larger g through dramatically enhancing $\omega_l''(0)$ and x_{zpf}.

IV. CONCLUSION

In conclusion, we propose a hybrid spin-optomechanical system to explore the single-photon-induced phonon blockade. We show that the statistical properties of the phonons can be controlled by the ancillary photons. More importantly, the resulted phonon blockade is completely switchable. This switchable behavior comes from the combined effect of the two ancillary cavity modes. We also demonstrate that the quantum effect of the phonon blockade can be strengthened

by adjusting the system parameters. In addition, the effect of the thermal phonon number on the phonon blockade is also discussed. It's shown that it requires to decrease the thermal noise to obtain the desired phonon blockade. Combined with the current single-photon technologies, our work offers a promising approach to realize the photon-controlled-phonon manipulation. Specifically, in analogy to the realization of a single-photon transistor where one photon can switch a signal containing multiple photons, our result makes it possible to perform single-photon-controlled phonon transistor on the basis of photon-controlled phonon statistics. In addition, these manipulation can be applied in the future hybrid photon-phonon quantum networks.

[1] M. Aspelmeyer, T. J. Kippenberg, and F. Marquardt, Rev. Mod. Phys. **86**, 1391 (2014); M. Aspelmeyer, P. Meystre, and K. Schwab, Phys. Today **65**, 29 (2012); P. Meystre, Ann. Phys. (Berlin) **525**, 215 (2013); F. Marquardt and S. M. Girvin, Physics **2**, 40 (2009); T. J. Kippenberg and K. J. Vahala, Science **321**, 1172 (2008).

[2] H. Xiong, L.-G. Si, X.-Y. Lü, X.-X. Yang, and Y. Wu, Sci. China: Phys., Mech. Astron. **58**, 1 (2015).

[3] C.-P. Sun and Y. Li, Sci. China: Phys., Mech. Astron. **58**, 1 (2015).

[4] A. D. O'Connell *et al.*, Nature (London) **464**, 697 (2010).

[5] J. D. Teufel, T. Donner, D. Li, J. W. Harlow, M. S. Allman, K. Cicak, A. J. Sirois, J. D. Whittaker, K. W. Lehnert, and R. W. Simmonds, Nature (London) **475**, 359 (2011).

[6] J. Chan, T. P. M. Alegre, A. H. Safavi-Naeini, J. T. Hill, A. Krause, S. Gröblacher, M. Aspelmeyer, and O. Painter, Nature (London) **478**, 89 (2011).

[7] J. B. Clark, F. Lecocq, R. W. Simmonds, J. Aumentado, and J. D. Teufel, Nature (London) **541**, 191 (2017).

[8] Y. X. Liu, A. Miranowicz, Y. B. Gao, J. Bajer, C. P. Sun, and F. Nori, Phys. Rev. A **82**, 032101 (2010).

[9] X. Wang, A. Miranowicz, H. R. Li, and F. Nori, Phys. Rev. A **93**, 063861 (2016).

[10] X.-W. Xu, A.-X. Chen, and Y.-X. Liu, Phys. Rev. A **94**, 063853 (2016).

[11] T. Ramos, V. Sudhir, K. Stannigel, P. Zoller, and T. J. Kippenberg, Phys. Rev. Lett. **110**, 193602 (2013).

[12] H. Seok and E. M. Wright, Phys. Rev. A **95**, 053844 (2017).

[13] H. Xie, C. G. Liao, X. Shang, M. Y. Ye, and X. M. Lin, Phys. Rev. A **96**, 013861 (2017).

[14] H. Xie, C. G. Liao, X. Shang, Z. H. Chen, and X. M. Lin, Phys. Rev. A **98**, 023819 (2018).

[15] H. Q. Shi, X. T. Zhou, X. W. Xun, and N. H. Liu, Sci. Rep. **8**, 2212 (2018).

[16] X.-Y. Lü, J.-Q. Liao, L. Tian, and F. Nori, Phys. Rev. A **91**, 013834 (2015).

[17] M. Wang, X.-Y. Lü, Y.-D. Wang, J. Q. You, and Y. Wu, Phys. Rev. A **94**, 053807 (2016).

[18] U. B. Hoff, J. Kollath-Bönig, J. S. Neergaard-Nielsen, and U. L. Andersen, Phys. Rev. Lett. **117**, 143601 (2016).

[19] T. J. Milburn, M. S. Kim, and M. R. Vanner, Phys. Rev. A **93**, 053818 (2016).

[20] F. Lecocq, J. B. Clark, R. W. Simmonds, J. Aumentado, and J. D. Teufel, Phys. Rev. X **5**, 041037 (2015).

[21] R. Riedinger, S. Hong, R. A. Norte, J. A. Slater, J. Shang, A. G. Krause, V. Anant, M. Aspelmeyer, and S. Gröblacher, Nature (London) **530**, 313 (2016).

[22] C. F. Ockeloen-Korppi, E. Damskägg, J.-M. Pirkkalainen, A. A. Clerk, M. J. Woolley, and M. A. Sillanpää, Phys. Rev. Lett. **117**, 140401 (2016).

[23] S. Hong, R. Riedinger, I. Marinković, A. Wallucks, S. G. Hofer, R. A. Norte, M. Aspelmeyer, and S. Gröblacher, Science **358**, 203 (2017).

[24] R. Riedinger, A. Wallucks, I. Marinković, C. Löschnauer, M. Aspelmeyer, S. Hong, and S. Gröblacher, Nature (London) **556**, 473 (2018).

[25] C. F. Ockeloen-Korppi, E. Damskägg, J.-M. Pirkkalainen, M. Asjad, A. A. Clerk, F. Massel, M. J. Woolley, and M. A. Sillanpää, Nature (London) **556**, 478 (2018).

[26] I. Marinković, A. Wallucks, R. Riedinger, S. Hong, M. Aspelmeyer, and S. Gröblacher, Phys. Rev. Lett. **121**, 220404 (2018).

[27] K. Stannigel, P. Komar, S. J. M. Habraken, S. D. Bennett, M. D. Lukin, P. Zoller, and P. Rabl, Phys. Rev. Lett. **109**, 013603 (2012).

[28] A. Imamoḡlu, H. Schmidt, G. Woods, and M. Deutsch, Phys. Rev. Lett. **79**, 1467 (1997).

[29] K. M. Birnbaum, A. Boca, R. Miller, A. D. Boozer, T. E. Northup, and H. J. Kimble, Nature (London) **436**, 87 (2005).

[30] P. Rabl, Phys. Rev. Lett. **107**, 063601 (2011).

[31] A. Kronwald, M. Ludwig, and F. Marquardt, Phys. Rev. A **87**, 013847 (2013).

[32] J.-Q. Liao and F. Nori, Phys. Rev. A **88**, 023853 (2013).

[33] H. Wang, X. Gu, Y.-X. Liu, A. Miranowicz, and F. Nori, Phys. Rev. A **92**, 033806 (2015).

[34] C. Santori, D. Fattal, J. Vuckovic, G. S. Solomon, and Y. Yamamoto, Nature (London) **419**, 594 (2002).

[35] S. V. Polyakov, A. Muller, E. B. Flagg, A. Ling, N. Borjemscaia, E. Van Keuren, A. Migdall, and G. S. Solomon, Phys. Rev. Lett. **107**, 157402 (2011).

[36] J. H. Prechtel, A. V. Kuhlmann, J. Houel, L. Greuter, A. Ludwig, D. Reuter, A. D. Wieck, and R. J. Warburton, Phys. Rev. X **3**, 041006 (2013).

[37] A. Kuhn, M. Hennrich, and G. Rempe, Phys. Rev. Lett. **89**, 067901 (2002).

[38] J. McKeever, A. Boca, A. D. Boozer, R. Miller, J. R. Buck, A. Kuzmich, and H. J. Kimble, Science **303**, 1992 (2004).

[39] M. Keller, B. Lange, K. Hayasaka, W. Lange, and H. Walther, Nature (London) **431**, 1075 (2004).

[40] J. E. Kennard, J. P. Hadden, L. Marseglia, I. Aharonovich, S. Castelletto, B. R. Patton, A. Politi, J. C. F. Matthews, A. G. Sinclair, B. C. Gibson, S. Prawer, J. G. Rarity, and J. L. O'Brien, Phys. Rev. Lett. **111**, 213603 (2013).

[41] A. Reiserer, S. Ritter, and G. Rempe, Science **342**, 1349 (2013).

[42] K. Xia, M. Johnsson, P. L. Knight, and J. Twamley, Phys. Rev. Lett. **116**, 023601 (2016).

[43] L. Neumeier, M. Leib, and M. J. Hartmann, Phys. Rev. Lett. **111**, 063601 (2013).

[44] L. Zhou, L.-P. Yang, Y. Li, and C. P. Sun, Phys. Rev. Lett. **111**, 103604 (2013).

[45] S. Baur, D. Tiarks, G. Rempe, and S. Dürr, Phys. Rev. Lett. **112**, 073901 (2014).

[46] I. Söllner, L. Midolo, and P. Lodahl, Phys. Rev. Lett. **116**, 234301 (2016).

[47] X.-Y. Lü, G.-L. Zhu, L.-L. Zheng, and Y. Wu, Phys. Rev. A **97**, 033807 (2018).

[48] X.-Y. Lü, L.-L. Zheng, G.-L. Zhu, and Y. Wu, Phys. Rev. Appl. **9**, 064006 (2018).

[49] J. D. Thompson, B. M. Zwickl, A. M. Jayich, F. Marquardt, S. M. Girvin, and J. G. E. Harris, Nature (London) **452**, 72 (2008).

[50] M. Bhattacharya, H. Uys, and P. Meystre, Phys. Rev. A **77**, 033819 (2008).

[51] S. J. M. Habraken, K. Stannigel, M. D. Lukin, P. Zoller, and P. Rabl, New J. Phys. **14**, 115004 (2012).

[52] Z.-L. Xiang, S. Ashhab, J. Q. You, and F. Nori, Rev. Mod. Phys. **85**, 623 (2013).

[53] G. Kurizki, P. Bertet, Y. Kubo, K. Molmer, D. Petrosyan, P. Rabl, and J. Schmiedmayer, Proc. Natl. Acad. Sci. USA **112**, 3866 (2015).

[54] R. N. Patel, C. J. Sarabalis, W. Jiang, J. T. Hill, and A. H. Safavi-Naeini, Phys. Rev. Appl. **8**, 041001 (2017).

[55] M.-A. Lemonde, S. Meesala, A. Sipahigil, M. J. A. Schuetz, M. D. Lukin, M. Loncar, and P. Rabl, Phys. Rev. Lett. **120**, 213603 (2018).

[56] O. Arcizet, V. Jacques, A. Siria, P. Poncharal, P. Vincent, and S. Seidelin, Nat. Phys. **7**, 879 (2011).

[57] S. D. Bennett, N. Y. Yao, J. Otterbach, P. Zoller, P. Rabl, and M. D. Lukin, Phys. Rev. Lett. **110**, 156402 (2013).

[58] J. Teissier, A. Barfuss, P. Appel, E. Neu, and P. Maletinsky, Phys. Rev. Lett. **113**, 020503 (2014).

[59] K. Jähne, C. Genes, K. Hammerer, M. Wallquist, E. S. Polzik, and P. Zoller, Phys. Rev. A **79**, 063819 (2009).

[60] W. J. Gu, G. X. Li, and Y. P. Yang, Phys. Rev. A **88**, 013835 (2013).

[61] Y.-D. Wang and A. A. Clerk, Phys. Rev. Lett. **110**, 253601 (2013).

[62] A. Nunnenkamp, V. Sudhir, A. K. Feofanov, A. Roulet, and T. J. Kippenberg, Phys. Rev. Lett. **113**, 023604 (2014).

[63] X.-Y. Lü, Y. Wu, J. R. Johansson, H. Jing, J. Zhang, and F. Nori, Phys. Rev. Lett. **114**, 093602 (2015).

[64] T.-S. Yin, X.-Y. Lü, L.-L. Zheng, M. Wang, S. Li, and Y. Wu, Phys. Rev. A **95**, 053861 (2017).

[65] M.-A. Lemonde, N. Didier, and A. A. Clerk, Nat. Commun. **7**, 11388 (2016).

[66] S. Guan, W. P. Bowen, C. Liu, and Z. Duan, Europhys. Lett. **119**, 58001 (2017).

[67] D. H. Santamore, A. C. Doherty, and M. C. Cross, Phys. Rev. B **70**, 144301 (2004).

[68] Y. Yanay and A. A. Clerk, New J. Phys. **19**, 033014 (2017).

[69] M. Ludwig, A. H. Safavi-Naeini, O. Painter, and F. Marquardt, Phys. Rev. Lett. **109**, 063601 (2012).

[70] N. E. Flowers-Jacobs, S. W. Hoch, J. C. Sankey, A. Kashkanova, A. M. Jayich, C. Deutsch, J. Reichel, and J. G. E. Harris, Appl. Phys. Lett. **101**, 221109 (2012).

[71] H. K. Li, Y.-C. Liu, X. Yi, C.-L. Zou, X.-X. Ren, and Y.-F. Xiao, Phys. Rev. A **85**, 053832 (2012).

[72] E. J. Kim, J. R. Johansson, and F. Nori, Phys. Rev. A **91**, 033835 (2015).

[73] T.-S. Yin, X.-Y. Lü, L.-L. Wan, S.-W. Bin, and Y. Wu, Opt. Lett. **43**, 2050 (2018).